Global and Planetary Change
January 2024, Volume 232, Pages 104324 (14p.)
https://doi.org/10.1016/j.gloplacha.2023.104324
https://archimer.ifremer.fr/doc/00865/97644/

Sea level and East Asian monsoon influenced chemical weathering records in the southern South China Sea over the past 21 ka

Zhao Hongchao [1], Liu Zhifei [1, *], Zhao Yulong [1]

[1] State Key Laboratory of Marine Geology, Tongji University, Shanghai 200092, China

* Corresponding author : Liu Zhifei, email address : lzhifei@tongji.edu.cn

Abstract :

High-resolution major element geochemistry of Core MD05–2892 from the lower Sunda Slope was analyzed to investigate the variation of chemical weathering records and its controlling factors in the southern South China Sea since the last glaciation. Chemical index of alteration (CIA) and SiO2/Na2O ratio were selected as chemical weathering proxies. The values of the proxies are higher during the last glaciation than during the Holocene. We attribute this to the provenance shift caused by sea level change. Provenance analysis indicates that the Malay Peninsula and Sumatra were the major sediment sources for the study region during the last glaciation, while the Indochina Peninsula has been the major source since the early Holocene. Accordingly, the weathering evolution analysis reveals increased physical erosion in the Malay Peninsula and Sumatra during enhanced East Asian summer monsoon rainfall, while increased chemical weathering in the Indochina Peninsula during the intensified monsoon rainfall. Therefore, the chemical weathering records of the deep-sea sediments in the southern South China Sea were regulated by monsoon rainfall-driven physical erosion in the Malay Peninsula and Sumatra during the last glaciation, while the records have been influenced by monsoon rainfall-induced chemical weathering in the Indochina Peninsula since the early Holocene. This study emphasizes that higher weathering values of the deep-sea sediments during the last glaciation could be related to the provenance variation driven by sea level change, rather than to enhanced chemical weathering in the same provenance.

Highlights

► Provenance of sediments off the Sunda Shelf has changed from glaciation to Holocene. ► Intensive chemical weathering occurred on Malay Peninsula/Sumatra during glaciation. ► Sea level and East Asian monsoon have jointly affected deep-sea weathering records.

Keywords : major elements, sea level, East Asian monsoon, chemical weathering, southern South China Sea, Last glaciation

1. Introduction

Chemical weathering of silicate rocks is a primary process at the Earth surface, which regulates global climate by transferring carbon from the atmosphere to the sedimentary reservoir over geologic timescales (Berner et al., 1983; Beaulieu et al., 2012; Deng et al., 2022; Brantley et al., 2023). Weathering products of silicate rocks are commonly used to assess chemical weathering intensity, because their geochemical compositions contain the climatic information during the weathering process (Galy and France-Lanord, 1999; Colin et al., 2006; Liu et al., 2007, 2009, 2012; Lupker et al., 2013). Abundant weathering products are produced on the land surrounding the South China Sea, especially in its southern region, where is currently characterized by high sediment runoff (Milliman et al., 1999), strong chemical weathering (Liu et al., 2012), and high CO_2 consumption by chemical weathering (Hartmann et al., 2009). Weathering products generated in the southern region and

transported to the sea by rivers are also important tracers for the studies of sea level change, because the southern South China Sea has the widest and gentlest Sunda Shelf in the low latitudes (Steinke et al., 2003, 2008; Hanebuth et al., 2011). Therefore, the southern South China Sea constitutes a key region to study the variation in chemical weathering records of the products and its controlling factors.

Previous studies of chemical weathering records have been conducted on river samples surrounding the southern South China Sea and on deep-sea core sediments (Liu et al., 2007, 2012; Wan et al., 2017; Jiwarungrueangkul et al., 2019a, 2019b; Sang et al., 2022). The geochemical analysis of river sediments on the Indochina Peninsula, the Malay Peninsula, Sumatra, and Borneo not only quantitatively reveals the degree of chemical weathering in the entire continental region, but also indicates that the monsoon climate with constant temperature and abundant rainfall is the main forcing factor of chemical weathering (Liu et al., 2007, 2012). The geochemical and mineral analyses of the deep-sea core sediments since the last glaciation are complicated. Chemical index of alteration (CIA) of Core SO18383-3 and smectite/(illite + chlorite) of Core MD05-2896 are lower during the last glaciation than during the Holocene, which is interpreted as lower chemical weathering in the Indochina Peninsula controlled by the East Asian summer monsoon during the last glaciation (Jiwarungrueangkul et al., 2019a; Sang et al., 2022). CIA of ODP Site 1143 and smectite/(illite + chlorite) of Core CG2 are higher during the last glaciation than during the Holocene, which is attributed to enhanced chemical weathering of shelf sediments exposed during the last glacial sea-level lowstand (Huang et al., 2016; Wan et al., 2017). However, higher smectite/(illite + chlorite) of Core MD05-2893 during the last glaciation than during the Holocene is interpreted as a difference in deep-sea sediment provenances (Jiwarungrueangkul et al., 2019b). During the last glacial sea-level lowstand, the North Sunda River and the Chao Phraya-Johore River were developed on the exposed Sunda Shelf (Molengraaff and Weber, 1921; Voris, 2000; Sathiamurthy and Voris, 2006), and these paleo-rivers directly transported terrigenous sediments from the western Sunda Shelf to the deep sea, while the deep-sea slope mainly preserve terrigenous sediments from the eastern Sunda Shelf during the Holocene sea-level highstand (Jiwarungrueangkul et al., 2019b). Thus, there are different interpretations for the variation of chemical weathering records in the southern South China Sea since the last glaciation, indicating that the underlying controlling mechanism for the variation in chemical weathering records is not clear. Further, the degree and the evolution of chemical weathering in the western region have not yet been reported.

To fill these research gaps, we selected Core MD05-2892 (almost overlapping with the location of Core MD05-2893) on the lower slope off the North Sunda River (Fig. 1) for the high-resolution major element analysis on carbonate-free samples. The objective is to study the influence of sea level change and East Asian monsoon evolution on the chemical weathering records of the deep-sea sediments.

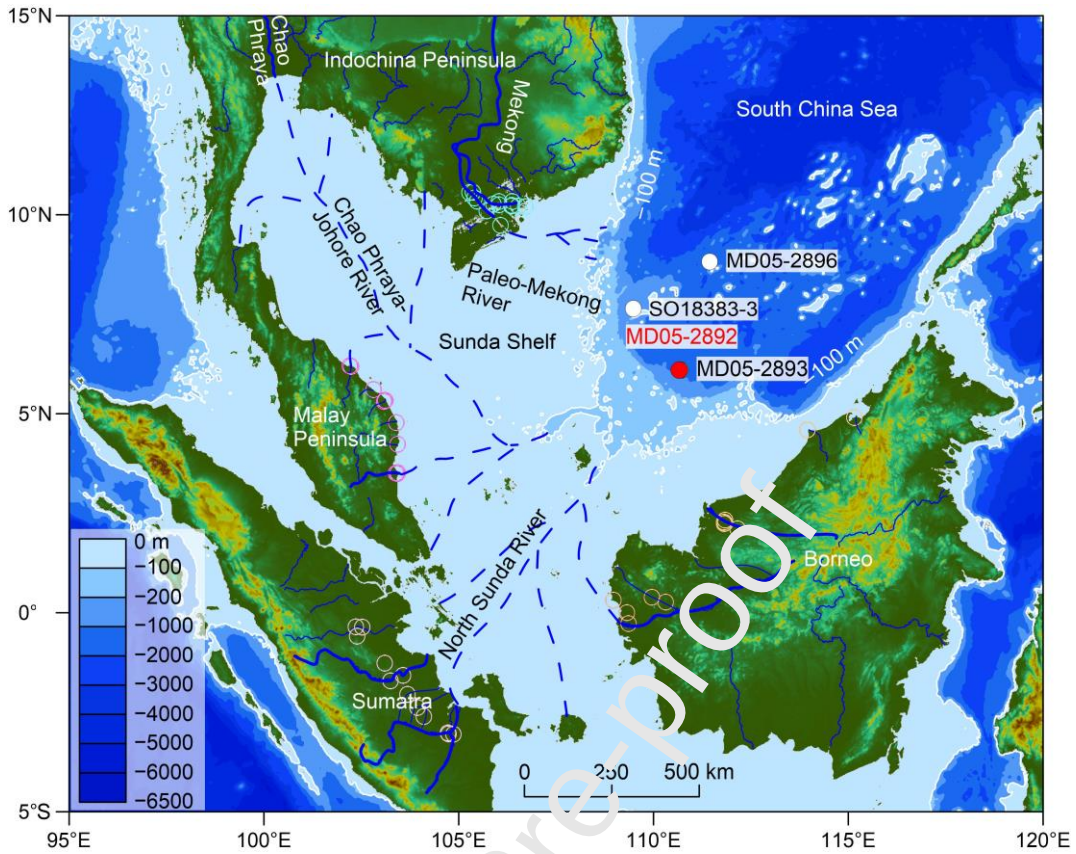

Fig. 1. Topography and bathymetry of the southern South China Sea showing the location of Core MD05-2892. The present −100 m isobath represents the average shoreline during the last glaciation. Blue dashed lines on the Sunda Shelf show paleo-river systems (North Sunda River, Chao Phraya-Johore River, and Paleo-Mekong River) developed during the last glaciation (Molengraaff and Weber, 1921; Voris, 2000; Sathiamurthy and Voris, 2006). Locations of river samples on the Indochina Peninsula, Borneo, the Malay Peninsula, and Sumatra (Liu et al., 2016) and of Cores SO18383-3 (Jiwarungrueangkul et al., 2019a), MD05-2893 (Jiwarungrueangkul et al., 2019b), and MD05-2896 (Sang et al., 2022) referred in this study are indicated. Note that the white circle of Core MD05-2893 is completely covered by the red circle of Core MD05-2892, because of almost the same locations of these two cores.

2. Material and Methods

Core MD05-2892 (6°06.12′N, 110°40.71′E; −1183 m water depth) was recovered from the lower Sunda Slope in the southern South China Sea during the MD147/Marco Polo-Images XII cruise in 2005 (Laj et al., 2005) (Fig. 1). The upper 13.7 m of the core was analyzed in this study. The lithology is dominated by olive gray homogeneous silty clay for the 0–3.6 m interval, and by dark gray laminated silty clay and clayey silt for the 3.6–13.7 m interval (Laj et al., 2005). The latter is characterized by millimeter-scale laminae, which are visually represented as interbedded dark and light gray layers (Fig. 2). The grain size of the dark-layer sediments (mainly as sand-containing clayey silt) is coarser than that of the light-layer sediments (mainly as silty clay), and the contact boundary between the dark and light layers is visually gradated (Zhao et al., 2023). The age model of the core was

established by using $\delta^{18}O$ records on *G. ruber* and AMS ^{14}C dating on planktonic foraminifera and wood debris (Supplementary Fig. S1) (Zhao et al., 2023). The ages of 0–3.6 m and 3.6–13.7 m intervals are 2.0–14.3 cal ka BP and 14.3–20.8 cal ka BP, respectively (Zhao et al., 2023). A total of 177 samples were selected for major element measurement.

Major elements were measured on fused glass beads by X-ray fluorescence (XRF) using a PANalytical Axios^{MAX} spectrometer at the State Key Laboratory of Marine Geology, Tongji University. Samples were first dried at 60°C and then grounded. Powder samples were reacted with 5% HCl to remove carbonate and then dried at 60°C. About 30–40 mg of the decarbonated samples were heated at 600°C to obtain the loss of ignition (LOI). Meanwhile, the decarbonated samples were fused and analyzed by the XRF method to obtain major element contents (Sang et al., 2022). ~0.7000 g of carbonate-free samples and ~7.000 g of $Li_2B_4O_7$ were uniformly mixed in a platinum crucible, and two drops of H_2O_2 and LiBr were added into the crucible. The platinum crucible was placed in the fusion machine, heated at 1050℃ for 8 min, and then cooled for 3 min to obtain glass beads for analysis. Chinese rock and sediment standards (GRS01, GSR03, GSR04, and GRS05) were analyzed to calculate the analytical accuracy (<10%) for major elements. Major elements were expressed as their oxides as absolute bulk contents of the carbonate-free samples (Supplementary Table D1).

3. Results

Major element distribution in Core MD05-2892 consists mainly of SiO_2 (54.9–82.5%), Al_2O_3 (9.9–20.8%), Fe_2O_3 (3.1–9.3%), K_2O (1.6–3.4%), and MgO (0.8–2.5%) with minor contents of TiO_2 (0.7–0.9%), Na_2O (0.5–0.9%), CaO (0.2–0.5%), P_2O_5 (0.1–0.2%), and MnO (0–0.2%) (Fig. 2). The contents of P_2O_5 and MnO are less than 0.2% and show independent variations. Therefore, these two elements are not further analyzed. The contents of the other eight elements show a clear glacial interglacial variation. Generally, Al_2O_3, K_2O, Fe_2O_3, and MgO show similar variation patterns, i.e., stable and high values during the Holocene and low values with high amplitude fluctuations during the last glaciation. The variations of SiO_2, Na_2O, CaO, and TiO_2 are inversely related to the variations of Al_2O_3, K_2O, Fe_2O_3, and MgO. On a short-term scale, the contents of the eight elements show two distribution patterns in the last glacial laminated sequence (Fig. 2). Content variations of SiO_2, Na_2O, and CaO are generally similar, but opposite to those of Al_2O_3, K_2O, Fe_2O_3, MgO, and TiO_2. The variations in elemental contents are correlated with dark-layer occurrences. Since the average thickness of dark layers (0.4 cm) is less than the thickness of measured samples (1 cm), the samples located at thick dark layers or light layers (>1 cm) are defined as dark-layer or light-layer samples, and the other samples are mixed-layer samples (Supplementary Table D1). In a typical dark layer, SiO_2, Na_2O, and CaO values show an upward and then a downward trend, while Al_2O_3, K_2O, Fe_2O_3, MgO, and TiO_2 show the opposite variation (Fig. 3). Statistically, SiO_2, Na_2O, and CaO values are high in dark layers and low in light layers, while Al_2O_3, K_2O, Fe_2O_3, MgO, and TiO_2 show the opposite characteristics (Fig. 4).

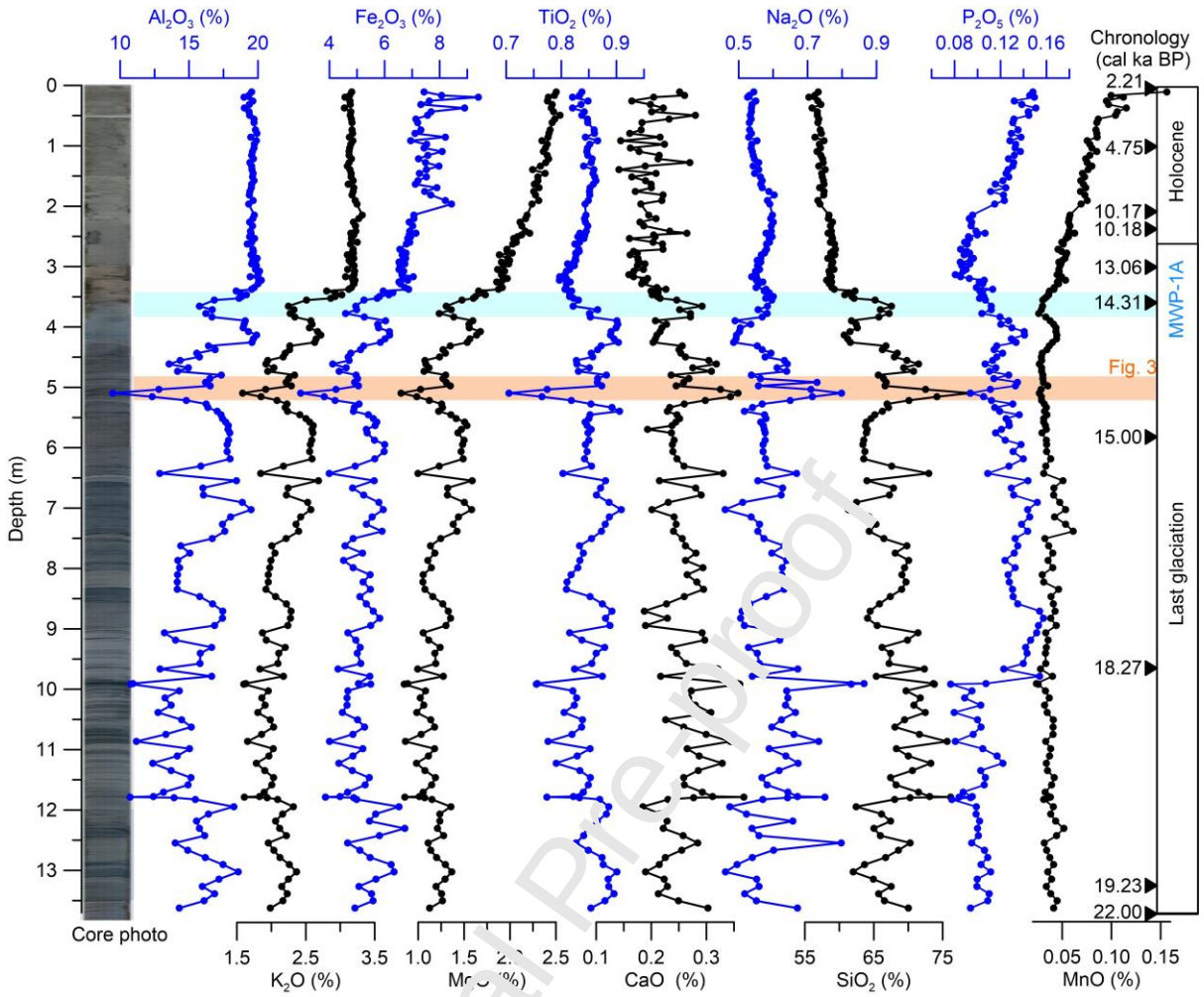

Fig. 2. Depth-scale variations of major element contents at Core MD05-2892 in the southern South China Sea. Core chronology was constructed by using 10 age control points of AMS ^{14}C combined with oxygen isotopes (Zhao et al., 2023). Yellow shaded zone presents a typical dark layer as shown for details in Fig. 3. Blue shaded zone shows the Meltwater Pulse 1A (MWP-1A) event inferred by sea level records in the Sunda Shelf (Hanebuth et al., 2000). Photo of Core MD05-2892 from Laj et al. (2005).

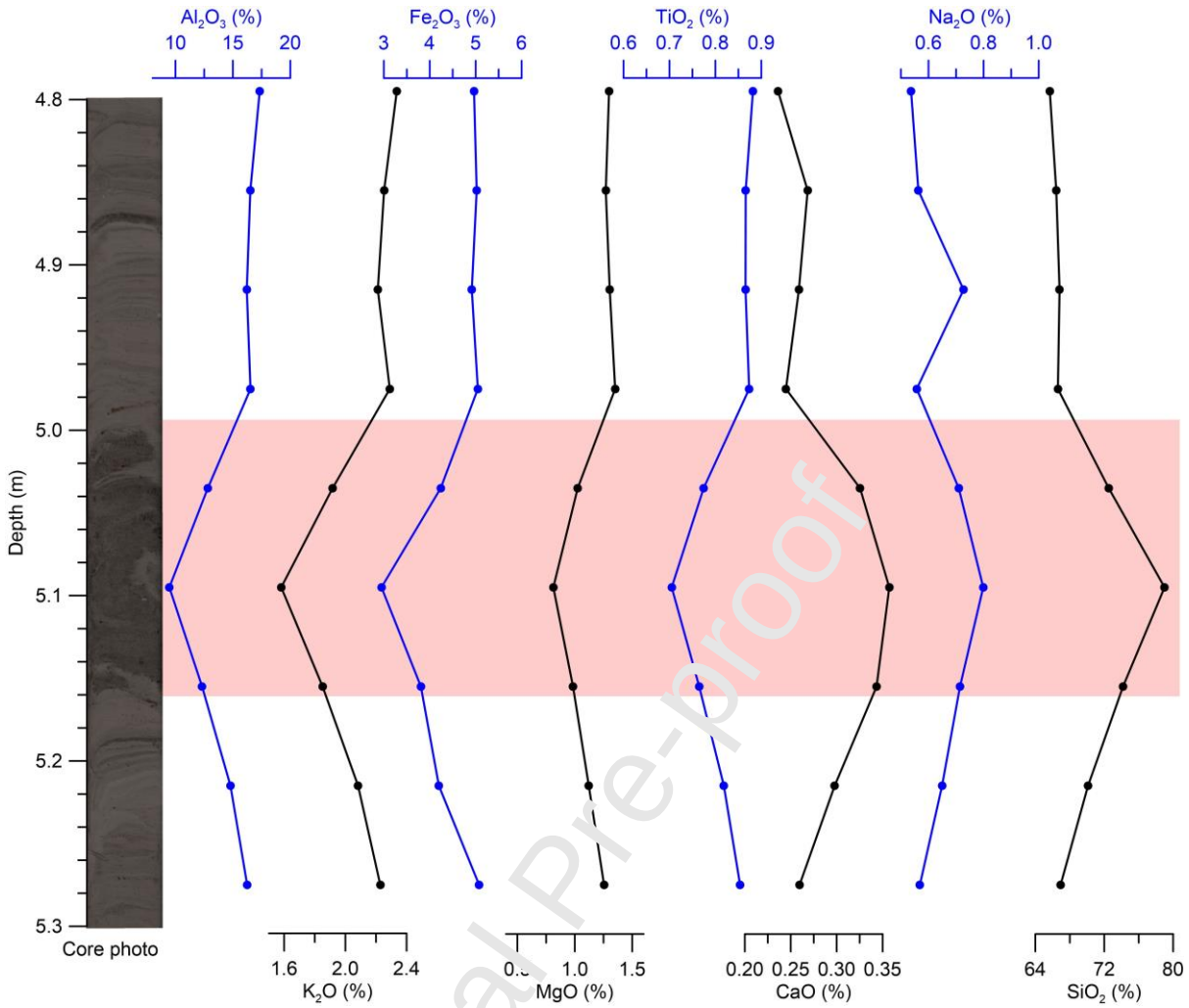

Fig. 3. Zoomed-in plots of major element contents in a typical dark layer (pink shaded zone) of Core MD05-2892 in the southern South China Sea. See Fig. 2 for the position at the core.

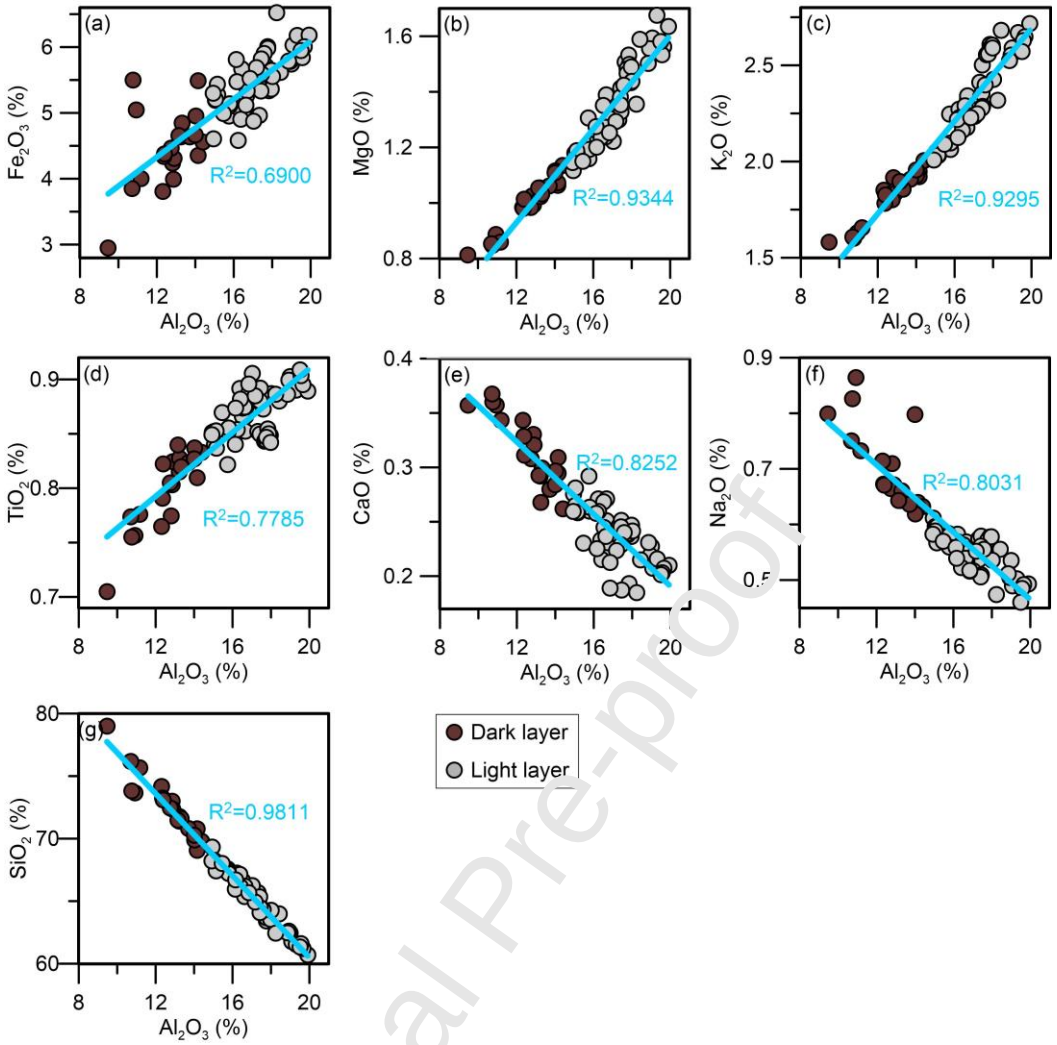

Fig. 4. Correlation plots of Al_2O_3 versus (a) Fe_2O_3, (b) MgO, (c) K_2O, (d) TiO_2, (e) CaO, (f) Na_2O, and (g) SiO_2 in light-layer and dark-layer sediments of Core MD05-2892 in the southern South China Sea during the last glacial 14.3–20.8 cal ka BP.

4. Discussion

4.1. Provenance analysis

Potential sources of deep-sea sediments are required before reconstructing the chemical weathering history (Liu et al., 2005; Wan et al., 2017). Clay-mineral data are typically used to analyze sediment sources of cores (Liu et al., 2016; Wan et al., 2017). Due to the almost same locations of Cores MD05-2892 and MD05-2893 (Fig. 1), the clay-mineral data of Core MD05-2893 could represent the clay-mineral characteristics of Core MD05-2892. Thus, clay-mineral data of Core MD05-2893 could be used to analyze the sediment sources of Cores MD05-2892 and MD05-2893. The clay mineral results of Core MD05-2893 have indicated that the terrigenous sediments were mixed materials from multiple sources (Fig. S2), and that the variations of terrigenous input since the last glaciation were primarily driven by sea level change (Jiwarungrueangkul et al., 2019b; Jiwarungrueangkul and Liu, 2021).

During the last glacial sea-level lowstand, terrigenous sediments were mainly transported from the western Sunda Shelf (i.e., the Malay Peninsula and Sumatra) via the Chao Phraya-Johore River and the North Sunda River (Jiwarungrueangkul et al., 2019b; Jiwarungrueangkul and Liu, 2021) (Fig. 1). Since the early Holocene, these two paleo-river systems have been rapidly flooded (Hanebuth et al., 2011), resulting in a relatively reduced terrigenous contribution from the western Sunda Shelf (Jiwarungrueangkul et al., 2019b; Jiwarungrueangkul and Liu, 2021). Meanwhile, more terrigenous sediments from the eastern Sunda Shelf (i.e., the Indochina Peninsula and northern Borneo) has been preserved in the deep sea (Jiwarungrueangkul et al., 2019b; Jiwarungrueangkul and Liu, 2021). Furthermore, the clay-mineral data shows that the illite+chlorite content and the illite chemical index with illite crystallinity in the core are close to the characteristics of the Indochina Peninsula river, instead of the Borneo rivers (Fig. S2) (Jiwarungrueangkul et al., 2019b). Considering the fluvial sediment discharge of the Mekong River (160×10^6 t/yr, Milliman and Syvitski, 1992) and of the northern Borneo rivers (42×10^6 t/yr, Liu et al., 2009), we assume that the Indochina Peninsula is a major sediment source for the southern South China Sea during the Holocene. These findings are supported by previous studies on the Sunda Slope (Steinke et al., 2003, 2008; Huang et al., 2016). Therefore, the major sediment source of Core MD05-2892 should be the Malay Peninsula and Sumatra rivers during the last glacial sea-level lowstand, and be the Indochina Peninsula river during the Holocene sea-level highstand.

Variation patterns of major element ratios between Cores MD05-2892 and MD05-2893 were compared to confirm the same sediment provenance of these two cores. Although the variation of elements could be related to many reasons, the variation reason of the same element at different cores in the same location should be the same. Due to almost the same locations of Cores MD05-2892 and MD05-2893 (Fig. 1), elemental variation reasons of the two cores should be the same. Therefore, without considering the reason of elemental variations, if elemental values and changes of the two cores are similar, the two cores have the same chemical composition (i.e., sedimentary composition). In other words, it's reasonable to use the clay-mineral conclusion of Core MD05-2893 as the provenance-analysis conclusion of Core MD05-2892. In terms of Core MD05-2892, the sum of SiO_2, Al_2O_3, and Fe_2O_3 is more than 80% (Fig. 2). As the dominant chemical compositions, these three elements of the two cores were selected for comparison. In addition, considering different analysis conditions of major elements in the two cores, SiO_2, Al_2O_3, and Fe_2O_3 were normalized by TiO_2. As a terrigenous element with a refractory nature, Ti has been widely used as a standard to eliminate interfering signals (Xie et al., 2014; Gebregiorgis et al., 2020; Zhao et al., 2023). SiO_2/TiO_2, Al_2O_3/TiO_2, and Fe_2O_3/TiO_2 ratios in Cores MD05-2892 and MD05-2893 are highly consistent in numerical and temporal variations, and the temporal variations of the elemental ratios are well correlated with sea level change (Fig. 5). There is a slight numerical deviation in the elemental ratios (~5 for SiO_2/TiO_2 ratio, ~1 for Al_2O_3/TiO_2 and Fe_2O_3/TiO_2 ratios) (Fig. 5), which may be related to different analytical methods. Major elements of Core MD05-2892 were measured on fused glass beads with decarbonated processes, whereas major elements of Core MD05-2892 were analyzed on compressed pellets

without decarbonation (Jiwarungrueangkul et al., 2019b). Variation patterns of the SiO_2/TiO_2 ratio are similar, and they are opposite to variations of the Al_2O_3/TiO_2 and Fe_2O_3/TiO_2 ratios (Fig. 5). The SiO_2/TiO_2 ratio shows high values with high amplitude fluctuations (67–112) during the last glacial sea-level lowstand, and remains stable at relatively low values (~70) during the Holocene sea-level highstand (Fig. 5). On the contrary, the Al_2O_3/TiO_2 and Fe_2O_3/TiO_2 ratios show highly fluctuating and low values (13–23 and 4–8, respectively) during the last glacial sea-level lowstand, and stable and high values (24 and 10, respectively) during the Holocene sea-level highstand (Fig. 5). Such similar variations of elemental ratios Cores MD05-2892 and MD05-2893 indicate the same geochemical characteristics, confirming that the terrigenous provenance of these two cores has been the same since the last glaciation.

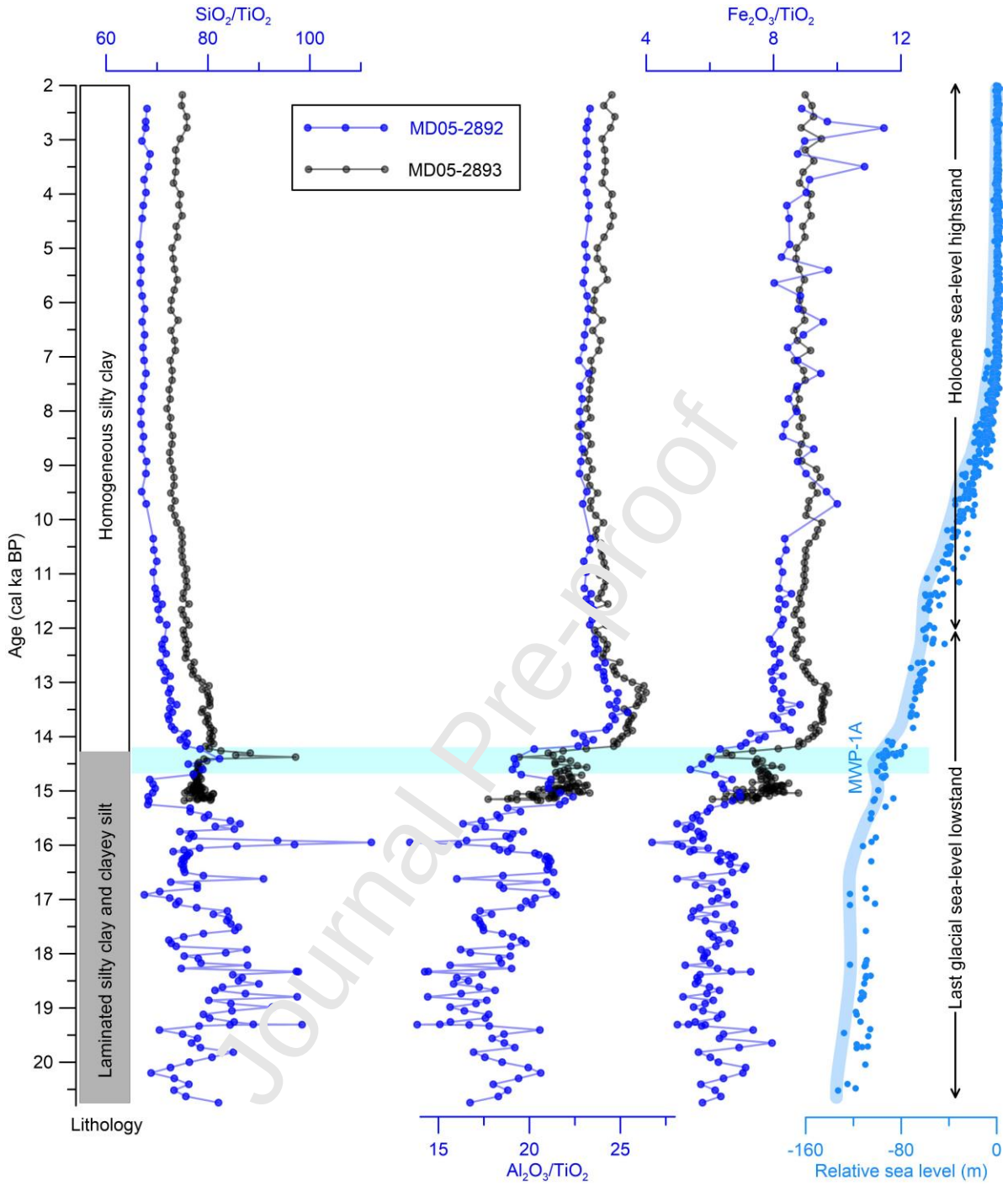

Fig. 5. Comparison of SiO_2/TiO_2, Al_2O_3/TiO_2, Fe_2O_3/TiO_2 ratios at Cores MD05-2892 and MD05-2893 in the southern South China Sea since the last glaciation. Relative sea-level data are included for correlation (Lambeck et al., 2014). Blue shaded zone shows the MWP-1A event inferred by sea level records in the Sunda Shelf (Hanebuth et al., 2000).

4.2. Chemical weathering intensity

After confirming the provenance of the terrigenous sediments, the chemical weathering intensity in the terrigenous provenance can be assessed using elemental indexes.

Theoretically, Na, Ca, Mg, and K are mobile elements during the chemical weathering process, while Si and Al are non-labile elements (Parker, 1970; Guo et al., 2018; Huang et al., 2021). Accordingly, some chemical weathering proxies have been proposed by previous studies, such as CIA (Nesbitt and Young, 1982) and Al/K (Hu et al. 2012; Clift et al., 2014; Jiwarungrueangkul et al., 2019b). In fact, Al variations are negatively correlated with Na and Ca variations, but positively correlated with K and Mg variations in Core MD05-2892 (Figs. 2–4). This indicates that Na and Ca elements in Core MD05-2892 are leaching, while K and Mg elements are not yet labile. Thus, CIA and SiO_2/Na_2O ratio were selected as chemical weathering indexes for Core MD05-2892. In addition, SiO_2/Al_2O_3 ratio was selected as a grain-size proxy. The combined analysis of these elemental ratios can reveal the chemical weathering intensity in the terrigenous provenance over the last 21 ka.

Elemental proxy variations of terrigenous sediments on the continental slope off the North Sunda River are well correlated with sea level change over the last 21 ka (Fig. 6). The CIA, SiO_2/Na_2O ratio, and SiO_2/Al_2O_3 ratio of Core MD05-2892 show highly variable and high values (72–83, 88–139, and 5–14, respectively) during the last glaciation, and stable and low values (80, 105, and 5, respectively) during the Holocene (Fig. 6). CIA values between 60 and 80 represent moderate chemical weathering, and CIA values above 80 indicate intensive chemical weathering (Nesbitt and Young, 1982; Liu et al., 2016; Guo et al., 2018). Accordingly, the elemental ratios of Core MD05-2892 reflect that deep-sea sediments were moderately to intensively weathered and coarse-grained during the last glaciation, and the terrigenous sediments were intensively weathered and fine-grained during the Holocene (Fig. 6). Due to the different grain sizes of the deep-sea sediments during these two periods (Fig. 6), it is difficult to directly compare the difference in the degree of chemical weathering between the Malay Peninsula and Sumatra during the last glaciation and the Indochina Peninsula during the Holocene.

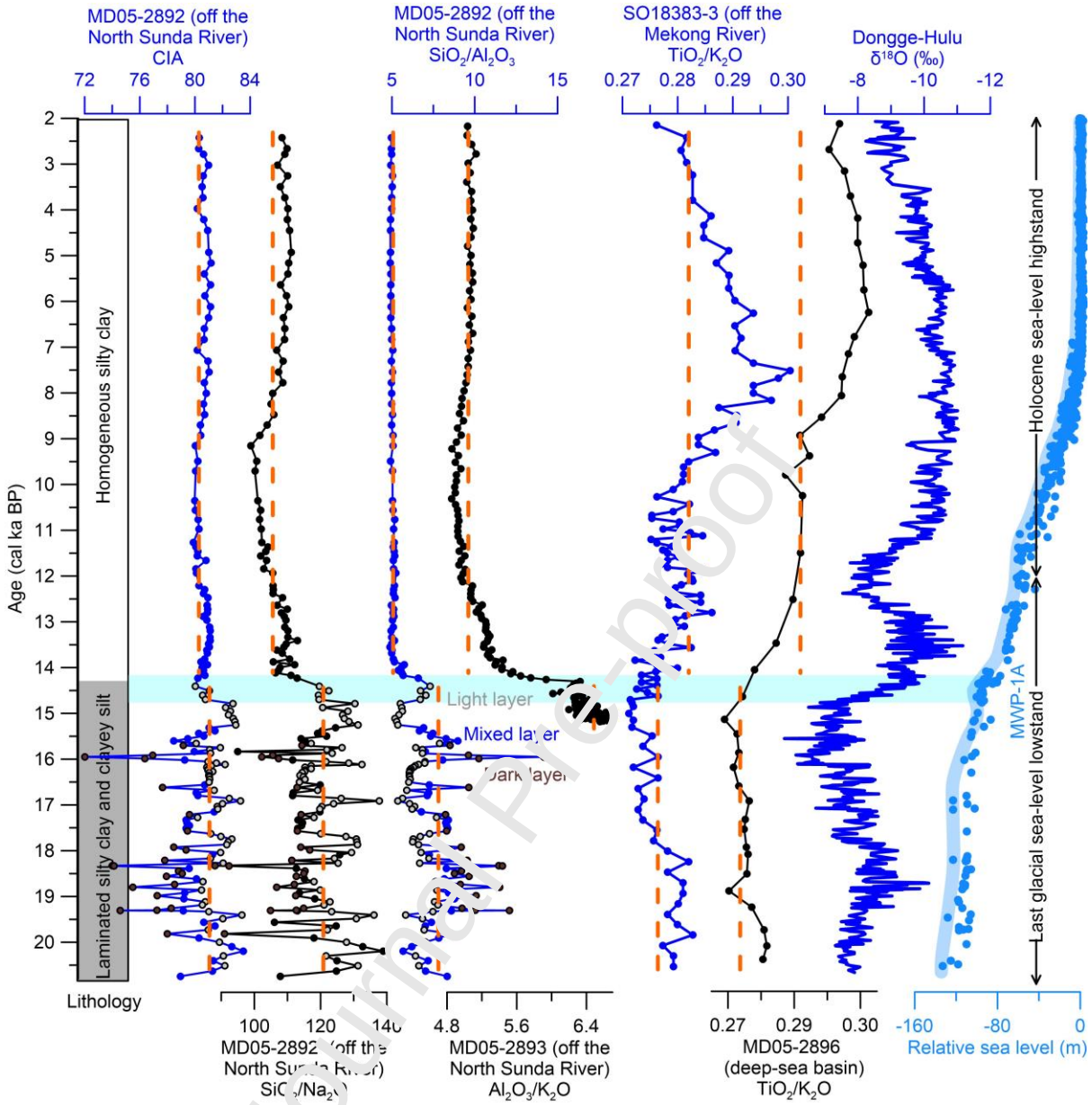

Fig. 6. Temporal variations in CIA, SiO_2/Na_2O ratio, and SiO_2/Al_2O_3 ratio of Core MD05-2892 and their comparison with Al_2O_3/K_2O ratio of Core MD05-2893 (Jiwarungrueangkul et al., 2019b), TiO_2/K_2O ratio of Core SO18383-3 (Jiwarungrueangkul et al., 2019a), and TiO_2/K_2O ratio of Core MD05-2896 (Sang et al., 2022) in the southern South China Sea over the past 21 ka. Yellow dashed lines show their average values. Light-grey, dark-brown, and blue/black circles of Core MD05-2892 in the last glacial laminated sequence represent light-layer, dark-layer, and mixed-layer sediments, respectively. Stalagmite $\delta^{18}O$ in Dongge-Hulu Caves (Cheng et al., 2016) and relative sea level (Lambeck et al., 2014) are included for correlation. Blue shaded zone shows the MWP-1A event inferred by sea level records in the Sunda Shelf (Hanebuth et al., 2000).

In order to compare the degree differences between different regions during the two periods, it is necessary to eliminate the effect of grain-size differences on the chemical weathering indexes. We follow the idea (Si/mobile element versus Si/Al) of Lupker et al.

(2013) to eliminate the grain-size effect. Specifically, SiO_2/Na_2O ratio values of Core MD05-2892 are higher during the last glaciation than during the Holocene, when the SiO_2/Al_2O_3 ratio is equal to 5 (Fig. 7a). This implies that the chemical weathering intensity in the Malay Peninsula and Sumatra during the last glaciation was higher than that in the Indochina Peninsula during the Holocene. The same feature is also shown in the correlation scatterplot of the CIA versus the SiO_2/Al_2O_3 ratio (Fig. 7b). The difference in CIA between these regions does not exceed 5 (Fig. 7b), which may be related to the fact that these regions are in the degree of intensive chemical weathering. Similar features are also observed in Southeast Asian river samples (Fig. 7). Because sediment source regions and climatic conditions are different, it's better to avoid interpreting the reason for the weathering degree differences between the Malay Peninsula/Sumatra and the Indochina Peninsula during different periods.

Interestingly, the CIA value of Core MD05-2892 during the last glaciation is close to CIA values of the Malay Peninsula and Sumatra rivers under the same grain-size condition (Fig. 7). This implies that the Malay Peninsula and Sumatra experienced intensive chemical weathering during both modern and last glacial periods, possibly related to the insensitivity of the tropics to temperature decreases during the last glaciation. This interpretation is supported by the pollen study in the southern South China Sea (Sun et al., 2000). Under the same sediment grain size condition, the CIA value of the core during the Holocene is consistent with the value of the Mekong River (Fig. 7), implying that the chemical weathering in the Indochina Peninsula has remained relatively consistent since the early Holocene. In addition, these geochemical characteristics of Core MD05-2892 also suggest that the previous provenance interpretation is reasonable (Fig. 7). Therefore, probably due to the insensitivity to temperature change in the tropics, the degree of chemical weathering in the Malay Peninsula and Sumatra during the last glacial and modern periods is similar, and the weathering degree in the Indochina Peninsula is consistent during the Holocene.

The value variations of chemical weathering intensities in Core MD05-2892 are clearly different during the last glaciation and Holocene. During the last glaciation, the chemical weathering and grain-size indexes of Core MD05-2892 show a large variation (Fig. 7). This reflects a large variation in grain sizes and chemical weathering intensities of terrigenous sediments delivered to the lower slope from the Malay Peninsula and Sumatra. Because of the large variation in terrigenous input, the chemical weathering indexes show a significant correlation with the grain-size proxy (Fig. 7). Specifically, the correlation coefficient (R^2) for CIA vs. SiO_2/Al_2O_3 and SiO_2/Na_2O vs. SiO_2/Al_2O_3 are 0.9338 and 0.4558, respectively (Fig. 7). Using the SiO_2/Al_2O_3 ratio, we classified the core into three grain-size units, i.e., fine-grained (the ratio <5), medium-grained (5–8), and coarse-grained (>8) units (Fig. 7). Such distinctly different characteristics of terrigenous input may be related to the short distance between the core site and the paleo-estuary of the North Sunda River and the Chao Phraya-Johore River during the last glaciation (Fig. 7). Under the short core-estuary distance condition (Zhao et al., 2023), both coarse-grained, moderately weathered terrigenous sediments and medium-grained, intensively weathered sediments from the Malay Peninsula and Sumatra could be transported to the deep sea. The average sedimentation rate of Core

MD05-2892 during the last glaciation (~170 cm/ka) was 6 times higher than the rate during the Holocene, indicating that a large number of terrigenous sediments was transported to the deep sea under the short core-estuary distance (Zhao et al., 2023). During the Holocene, the elemental ratios show an insignificant correlation with the grain-size proxy (Fig. 7). Specifically, the correlation coefficient (R^2) for CIA vs. SiO_2/Al_2O_3 and SiO_2/Na_2O vs. SiO_2/Al_2O_3 are 0.1967 and 0.1709, respectively (Fig. 7). This may be related to the long core-estuary distance during the Holocene, which makes it difficult for coarse-grained sediments to be transported to the deep sea (Zhao et al., 2023). Therefore, the core-estuary distance was short during the last glaciation, and the Malay Peninsula and Sumatra supplied a large amount of coarse-grained, moderately weathered sediments and medium-grained, intensively weathered sediments to the deep-sea slope, resulting in a large variation in chemical weathering proxies. The core-estuary distance is long during the Holocene, and the Indochina Peninsula supplied a small amount of fine-grained, intensively weathered sediments to the deep sea, resulting in a small variation in chemical weathering values.

Due to different formation mechanisms of light-layer (medium-grained and intensively weathered) sediments and dark-layer (coarse-grained and moderately weathered) sediments (Zhao et al., 2023), we selected chemical weathering proxies of light-layer sediments to study the silicate weathering history in the Malay Peninsula and Sumatra during the last glaciation. The formation of dark-layer sediments was related to hyperpycnal flow driven by strong hydrodynamic conditions, while light-layer formation was related to hemiplegic dispersal under weak hydrodynamic conditions (Zhao et al., 2023). In addition, the light-layer sediments belong to the same grain-size unit, providing the opportunity to reduce the effect of grain size on the elemental ratios. Therefore, CIA (average 82) of light-layer sediments during the last glaciation indicate the intensive chemical weathering in the Malay Peninsula and Sumatra at the meantime. CIA (average 81) of deep-sea sediments during the Holocene indicate the intensive chemical weathering in the Indochina Peninsula.

The above discussion is only an opinion based on the analysis of Core MD05-2892. In order to comprehensively understand the chemical weathering intensity in the source regions surrounding the southern South China Sea since the last glaciation, we compared the elemental characteristics of sediments on different geomorphic units in the deep sea (Fig. 7). We divided three geomorphic units in the southern South China Sea, namely the continental slope off the North Sunda River, the continental slope off the Mekong River, and the deep-sea basin (Fig. 7). For each geomorphic unit, we selected core sediments with high-resolution elemental data. Specifically, elemental ratios of Cores MD05-2896 (Sang et al., 2022), SO18383-3 (Jiwarungrueangkul et al., 2019a), and MD05-2892 represent sedimentary features of the deep-sea basin, the continental slope off the Mekong River, and the continental slope off the North Sunda River, respectively. Data quality assessment is required prior to data comparison. The analysis materials for the major elements in Core SO18383-3 are bulk samples (Jiwarungrueangkul et al., 2019a), which would result in Na and Ca elements being affected by NaCl and $CaCO_3$, respectively. Thus, the SiO_2/Na_2O ratio and CIA of Core SO18383-3 are not included in the discussion. The analysis materials of Core MD05-2896 and MD05-2892 are samples with NaCl and $CaCO_3$ removed, and they follow the same

experimental procedure. Therefore, the SiO_2/Na_2O ratio and CIA of these two cores can be compared. Since the SiO_2/Al_2O_3 ratio is not affected by NaCl and $CaCO_3$, the SiO_2/Al_2O_3 ratios of all three cores can be compared for analysis.

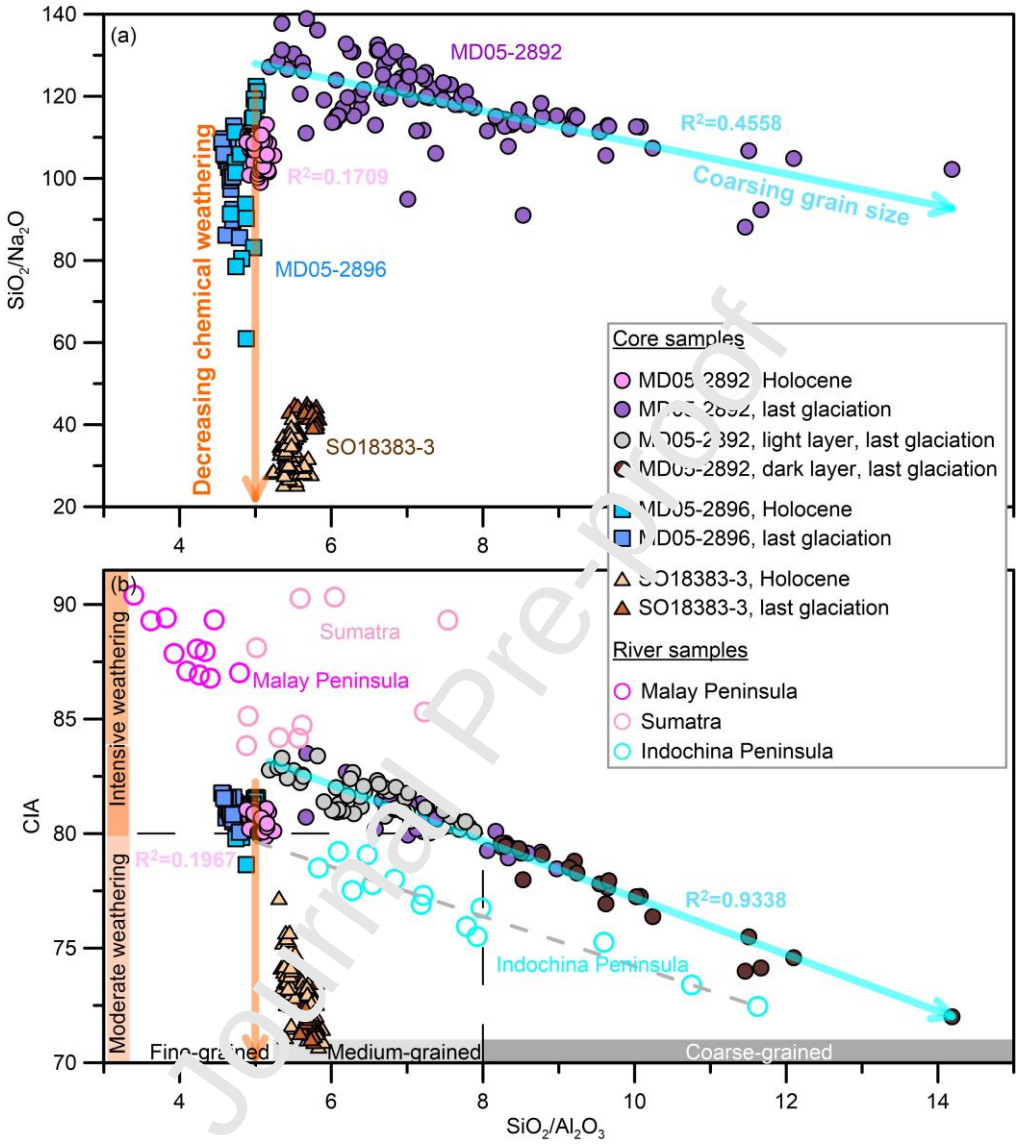

Fig. 7. Correlation plots of SiO_2/Al_2O_3 versus (a) SiO_2/Na_2O and (b) CIA of Core MD05-2892 in the southern South China Sea since the last glaciation. The elemental ratios of river samples and Cores SO18383-3 and MD05-2896 (Liu et al., 2016; Jiwarungrueangkul et al., 2019a; Sang et al., 2022) are included for comparison.

After comparing the elemental characteristics of three typical cores, we found that the chemical weathering intensity of terrigenous sediments is similar on different geomorphic units (Fig. 7). For the continental slope off the North Sunda River, as discussed previously, chemical weathering indexes during the last glaciation indicate the intensive chemical weathering in the Malay Peninsula and Sumatra, while the indexes during the Holocene reflect the intensive chemical weathering in the Indochina Peninsula (Fig. 7). For the

deep-sea basin, the elemental data of Core MD05-2896 almost overlap during the last glaciation and during the Holocene, and these data also overlap with Core MD05-2892 data during the Holocene (Fig. 7). This implies that the provenance of terrigenous sediments in the deep-sea basin was mainly from the Indochina Peninsula and the terrigenous source was unaffected by sea level change. This interpretation is consistent with the previous study (Sang et al., 2022). In addition, the grain-size-proxy values of Core MD05-2896 have been stable since the last glaciation (Fig. 7), implying that the hydrodynamics of the deep-sea basin were relatively stable. Without the influence of provenance shifts and grain-size differences, the chemical weathering intensity of terrigenous sediments on the deep-sea basin reflects the intensive chemical weathering in the Indochina Peninsula since the last glaciation (Fig. 7). For the continental slope off the Mekong River, the provenance of terrigenous sediments from Core SO18383-3 has been the Indochina Peninsula since the last glaciation (Jiwarungrueangkul et al., 2019a). The grain-size-proxy values of Core SO18383-3 range between 5 and 6 during the last glaciation and the Holocene (Fig. 7). Without the clear effect of the provenance change and grain-size difference, the elemental variations of sediments on the continental slope off the Mekong River reflect that the chemical weathering intensity in the Indochina Peninsula during the last glaciation was lower than during the Holocene (Fig. 6). Although the chemical weathering intensity during the last glaciation was relatively lower than that during the Holocene, the Indochina Peninsula is in a degree of intensive chemical weathering during these two periods (Fig. 7b). Therefore, during the last glaciation, the chemical weathering proxies of terrigenous sediments on the slope off the North Sunda River reflect the intensive chemical weathering in the Malay Peninsula and Sumatra, and the indexes on the deep-sea basin and on the slope off the Mekong River reflect the intensive chemical weathering in the Indochina Peninsula. During the Holocene, the indexes of deep-sea sediments on all geomorphic units reflect the intensive chemical weathering in the Indochina Peninsula.

4.3. Controlling factors for chemical weathering records

On the glacial-interglacial scale, the chemical weathering index of terrigenous sediments on the slope off the North Sunda River shows that the chemical weathering intensity in the silicate provenances was higher during the last glaciation than during the Holocene (Fig. 6). Such a variation is opposite to the general evolution of the East Asian summer monsoon proxy (stalagmite $\delta^{18}O$ in Dongge-Hulu Caves) (Fig. 6), which is strange but reasonable. The glacial-interglacial variation in chemical weathering proxies may be related to the provenance shift due to sea level change (Fig. 7). During the last glacial sea-level lowstand, the North Sunda River and the Chao Phraya-Johore River transported highly weathered products from the Malay Peninsula and Sumatra to the deep-sea slope (Jiwarungrueangkul et al., 2019b; Jiwarungrueangkul and Liu, 2021), leading to high weathering values. However, the sediment contribution from the Malay Peninsula and Sumatra has been decreased dramatically since the sea level rise (Steinke et al., 2003, 2008; Huang et al., 2016; Jiwarungrueangkul et al., 2019b). During this period, the sediment contribution from the Indochina Peninsula increases

relatively (Liu et al., 2005; Huang et al., 2016; Wan et al., 2017; Jiwarungrueangkul et al., 2019b; Jiwarungrueangkul and Liu, 2021), resulting in relatively low values of chemical weathering indexes in the deep-sea slope. Therefore, variations in the chemical weathering indexes in the lower slope off the North Sunda River on the glacial-interglacial scale reflect the provenance shift of deep-sea sediments due to sea level change, rather than the evolution of silicate weathering in the same source region (Figs. 6 and 7).

On short-term scales during the last glaciation, the chemical weathering indexes of light-layer sediments and the rainfall proxy of the East Asian summer monsoon show similar variations (Fig. 8). Specifically, the interval of decreased weathering indexes corresponds to enhanced monsoon rainfall (decreased stalagmite $\delta^{18}O$ values in the Dongge-Hulu Cave and Borneo), while the increased indexes correlate with weakened rainfall (Fig. 8). The reason for this phenomenon may be related to physical erosion in the Malay Peninsula and Sumatra. Enhanced rainfall possibly led to increased physical erosion in this region during the last glaciation, and the silicate were rapidly eroded and transported to the deep sea before adequate chemical weathering could occur. On the contrary, when the monsoon rainfall was weakened, the physical erosion was reduced, and the silicate minerals possibly had enough time to experience intensive chemical weathering. Our opinion was supported by the nearby site (Core MD01-2385) in the tropical region (Yu et al., 2023). CIA of Core MD01-2385 showed lower values during the strengthened precipitation period and higher values during the weak rainfall stage (Yu et al., 2023). The previous study interpreted this phenomenon as increased precipitation enhanced both the physical erosion rate and sediment transport efficiency, leading to less time for sediments to be strongly chemically weathered in soils, and hence driving the delivery of detrital minerals characterized by a lower degree of chemical weathering (Yu et al., 2023). Furthermore, in the previous study (Core CG2, located on the continental slope off the Sunda Shelf), higher values of the Si/Al ratio were used to indicate higher terrigenous and freshwater inputs from the North Sunda River (Huang et al., 2019). Following the same idea, the SiO_2/Al_2O_3 ratio of Core MD05-2892 at the same grain-size (light-layer sediments, medium grained) was used to indicate the variation of terrigenous and freshwater inputs. Accordingly, higher SiO_2/Al_2O_3 ratios indicated higher terrigenous and freshwater inputs during the intensified summer monsoon (Fig. 8). In other words, the intensified summer monsoon led to increased physical erosion in the Malay Peninsula and Sumatra during the last glaciation. This conclusion is supported by a previous study in the same region (Huang et al., 2016). Based on clay-mineral analysis of nearby Core CG2, the previous study suggested that periods of strong monsoon rainfall were associated with the intensified erosion on the Sunda Shelf during the last glaciation (Huang et al., 2016). It's important to note that the relative variation in chemical weathering in the Malay Peninsula and Sumatra was related to physical erosion variations on short-term scales within the last glaciation, but the overall state of chemical weathering in this region was intensive (CIA>80) throughout the last glaciation (Fig. 8). Although the exposed shelf may be eroded during the last glaciation, we believe that the eroded shelf contributed less to the deep-sea sediments. Because the chemical weathering degree of pre-existing sediments on the exposed shelf was generally high (Wan et al., 2017), physical erosion of such highly weathered

sediments would result in increased, rather than decreased CIA values (Fig. 8). Therefore, relative variations of chemical weathering intensities in the Malay Peninsula and Sumatra on short-term scales during the last glaciation were associated with physical erosion changes driven by East Asian summer monsoon evolution.

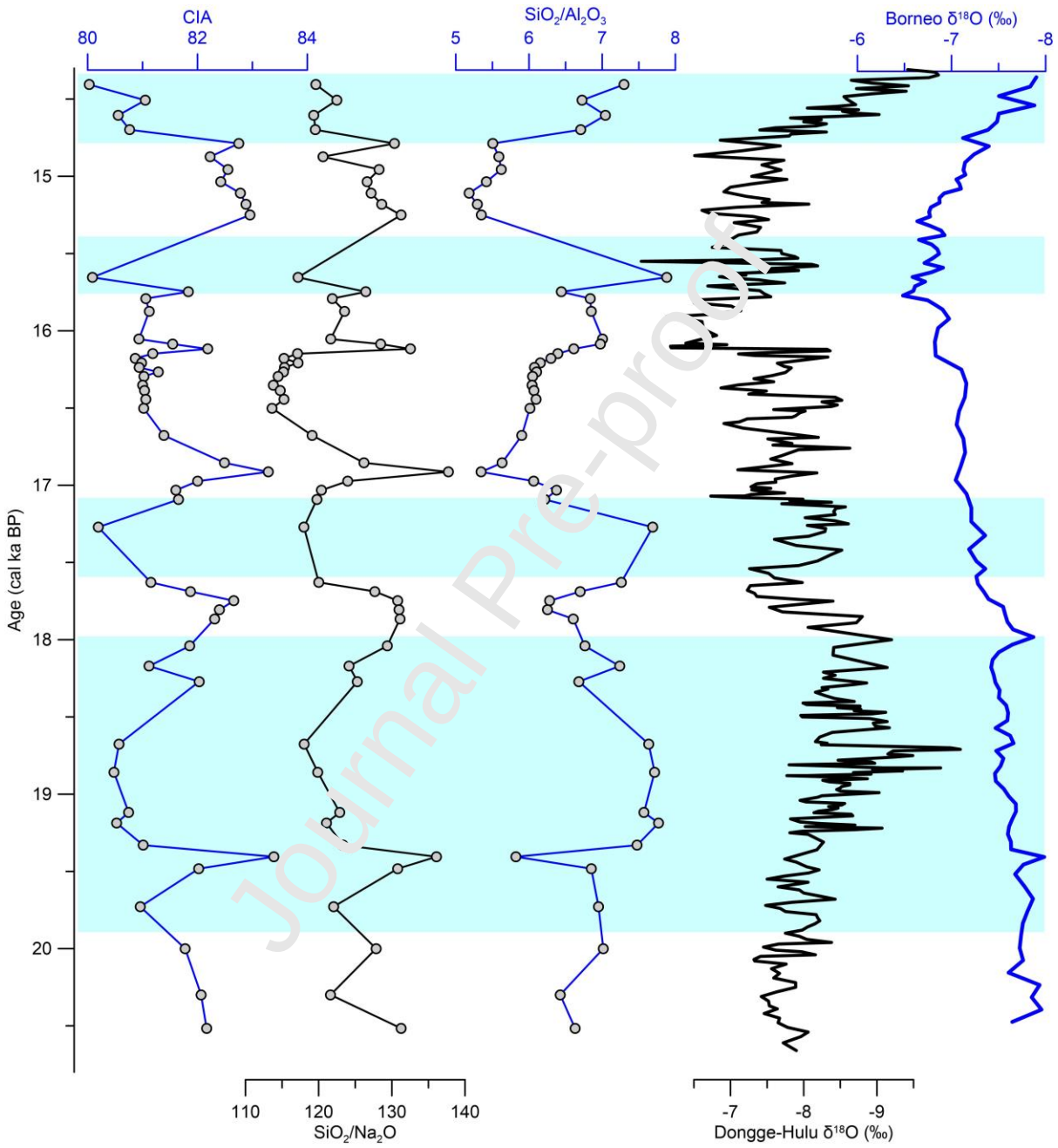

Fig. 8. Temporal variations in CIA, SiO_2/Na_2O ratio, and SiO_2/Al_2O_3 ratio of light-layer sediments from Core MD05-2892 in the southern South China Sea and their comparison with stalagmite $\delta^{18}O$ in Dongge-Hulu caves (Cheng et al., 2016) and the Borneo (Partin et al., 2007) during the last glacial 14.3–20.8 cal ka BP. Blue shaded zones show intervals of decreased CIA and SiO_2/Na_2O ratio.

On short-term scales during the Holocene, the chemical weathering indexes and the

monsoon rainfall proxy show opposite trends (Fig. 9). The decreased values of the weathering indexes in Core MD05-2892 occur during weakened monsoon rainfall (Fig. 9). The indexes indicate that the chemical weathering in the Indochina Peninsula was weakened during the 9.0–12.5 cal ka BP. This feature might be related to a cooling on the Asian continent (Sun et al., 2005; Zhao et al., 2006), which was associated with an interval of a weakened summer monsoon intensity (Wang et al., 2001; Dykoski et al., 2005) as an effect of the Younger Dryas (YD) cold period (Stuiver et al., 1995). The small variation of CIA might be related to the small effect of the YD on the tropical region, which is reflected as inconspicuous changes of the Borneo stalagmite $\delta^{18}O$ (Partin et al., 2007). The duration of the weak weathering event recorded in Core MD05-2892 is longer than that of the Younger Dryas (Fig. 9), which might be related to the prolonged response of chemical weathering to the weaken rainfall in the Indochina Peninsula. Previous studies in the southern South China Sea have also interpreted such variations of chemical weathering in the Indochina Peninsula as the effect of a decrease in summer monsoon rainfall during the YD (Jiwarungrueangkul et al., 2019a). In addition, the increased values of the weathering indexes correspond to enhanced monsoon rainfall (Fig. 9). This reflects that the strong rainfall promotes chemical weathering in the Indochina Peninsula. Therefore, the Indochina Peninsula during the Holocene is characterized by chemical weathering driven by East Asian summer monsoon evolution.

On short-term scales, the chemical weathering indexes of Core MD05-2892 respond differently to heavy rainfall between the last glaciation and the Holocene (Figs. 8 and 9). This indicates that the silicate weathering processes in the Malay Peninsula and Sumatra and in the Indochina Peninsula show different response patterns to heavy rainfall. This interpretation is also supported by records from other study areas. For example, the Taiwan is dominated by enhanced physical erosion during periods of heavy rainfall (Hu et al., 2012), while the Irrawaddy River basin is characterized by enhanced chemical weathering during heavy rainfall (Colin et al., 2006). The Mekong River basin in the Indochina Peninsula and Irrawaddy River basins are characterized by a large plain topography, while the Malay Peninsula, Sumatra, and Taiwan are marked by a large mountain topography. Therefore, possibly due to the different topography, the chemical weathering in different regions shows different response patterns to heavy monsoon rainfall.

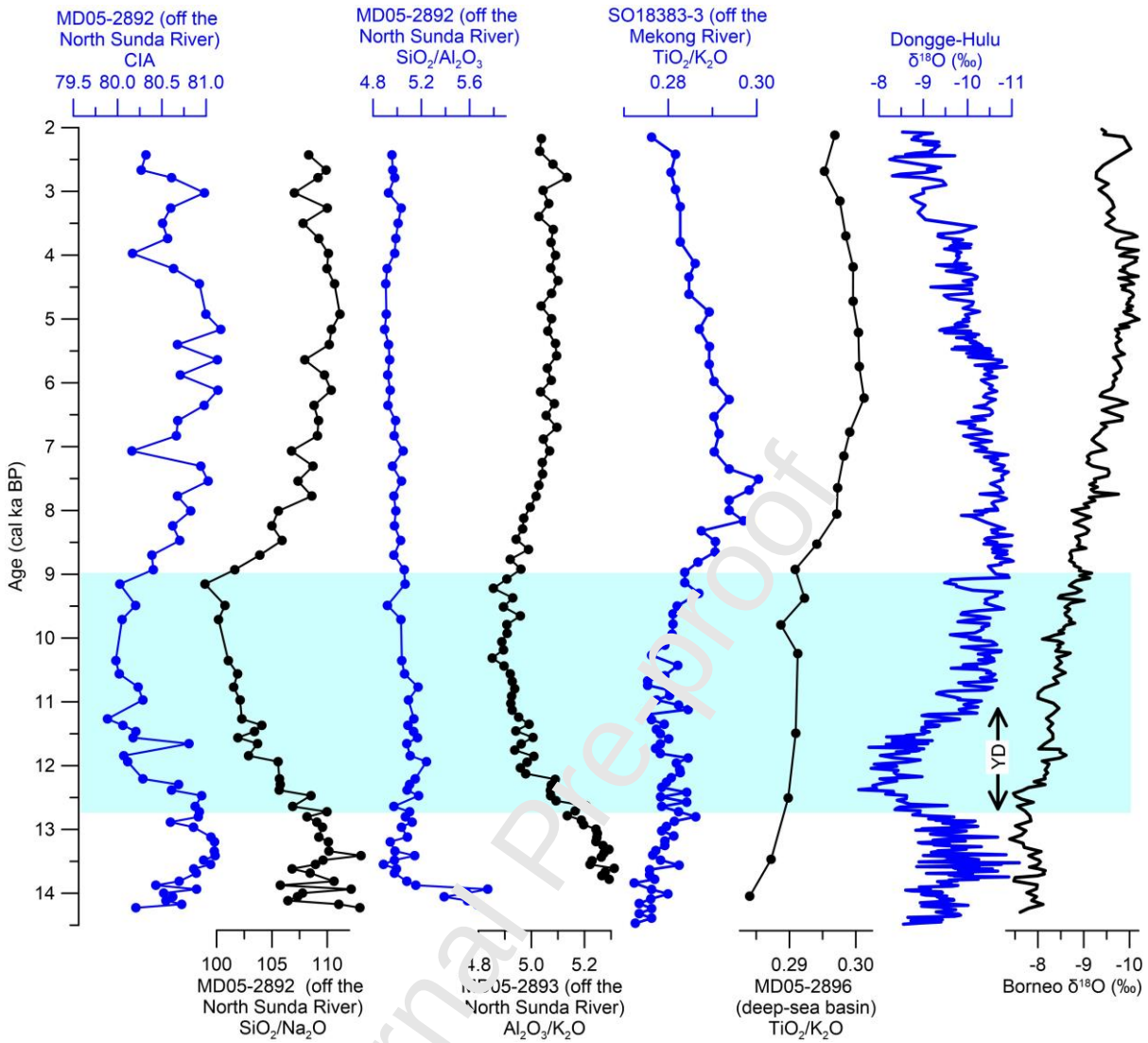

Fig. 9. Temporal variations in CIA, SiO_2/Na_2O ratio, and SiO_2/Al_2O_3 ratio of Core MD05-2892 in the southern South China Sea and their comparison with stalagmite $\delta^{18}O$ in Dongge-Hulu Caves (Cheng et al., 2016) and the Borneo (Partin et al., 2007) over the past 14.5 ka. Elemental ratios at Cores MD05-2893, SO18383-3, and MD05-2896 are included for comparison (Jiwarungrueangkul et al., 2019a, 2019b; Sang et al., 2022). Blue shaded zone shows the interval of decreased CIA and SiO_2/Na_2O ratio. Younger Dryas (YD, Stuiver et al., 1995) is indicated.

Comparing the chemical weathering index of Core MD05-2892 with those of other cores, we found that the chemical weathering intensity of terrigenous sediments on different geomorphic units in the deep sea of the southern South China Sea responded differently to the evolution of the East Asian summer monsoon since the last glaciation (Fig. 6). For the continental slope off the Mekong River and the deep-sea basin, the weathering intensity of terrigenous sediments was controlled only by the chemical weathering in the Indochina Peninsula driven by the monsoon rainfall (Fig. 6). For the continental slope off the North Sunda River, the intensity has been regulated by sea level change and monsoon evolution since the last glaciation. During the last glaciation, enhanced monsoon rainfall increased the

physical erosion in the Malay Peninsula and Sumatra (Fig. 8). During the Holocene, heavy rainfall increases chemical weathering in the Indochina Peninsula (Fig. 9).

To sum up, this research shows that the Malay Peninsula and Sumatra experienced intensive chemical weathering during the last glaciation, and the silicate weathering history in this region was characterized by physical erosion variations regulated by the East Asian monsoon evolution. This finding fills a gap in research of weathering processes in this region during the last glacial period. Additionally, this work presents that chemical weathering in the Indochina Peninsula has been influenced by the monsoon evolution since the early Holocene. This finding is consistent with the previous investigations in this region (Huang et al., 2016; Jiwarungrueangkul et al., 2019a, 2019b; Jiwarungrueangkul and Liu et al., 2021; Sang et al., 2022). More importantly, this study emphasizes that the provenance shift driven by sea level change could cause higher weathering degrees of deep-sea sediments during the last glaciation than during the Holocene. This finding is helpful to study the chemical weathering history based on global deep-sea sediments. Previous studies found that the last glacial sediments were more weathered than Holocene sediments in the deep-sea environment, and they attributed this to enhanced chemical weathering during the last glaciation (Huang et al., 2016; Wan et al., 2017; Xu et al., 2017). However, this study suggests that more weathered sediments in the deep-sea environment during the last glaciation could be related to the provenance shift due to sea level change, rather than to enhanced chemical weathering in the same source region during the last glaciation. Therefore, chemical weathering reconstruction based on deep-sea sediment records should be more cautious in future work.

5. Conclusions

High-resolution major-element geochemistry on decarbonated samples of Core MD05-2892 on the continental slope off the North Sunda River was analyzed to elucidate the variation of chemical weathering records and its controlling factors in southern South China Sea over the past 21 ka. We have the following main conclusions:

(1) The deep-sea sediments on the slope off the North Sunda River were mainly derived from the Malay Peninsula and Sumatra during the last glaciation, while the terrigenous sediments have been mainly from the Indochina Peninsula since the early Holocene.

(2) The values of chemical weathering indexes (i.e., CIA and SiO_2/Na_2O ratio) in the deep-sea sediments reveal that the Malay Peninsula and Sumatra was characterized by intensive chemical weathering during the last glaciation, and the Indochina Peninsula is marked by intensive chemical weathering during the Holocene.

(3) The evolution of chemical weathering proxies in the deep-sea sediments over the last 21 ka is influenced by sea level change and the East Asian summer monsoon evolution. Sea level change led to a shift in the deep-sea sediment provenance from the Malay Peninsula and Sumatra during the last glaciation to the Indochina Peninsula during the Holocene. Intensified summer monsoon led to increased physical erosion in the Malay Peninsula and Sumatra during the last glaciation, while enhanced summer monsoon has resulted in enhanced chemical weathering in the Indochina Peninsula since the early Holocene.

Data availability

Research data used in this study are provided in Supplementary Table D1.

Declaration of competing interest

The authors declare that they have no known competing financial interests or personal relationships that could appear to have influenced the work reported in this paper.

Acknowledgments

We would like to thank the crew and scientists aboard the R/V Marion Dufresne for collecting the sediment core during the MD147/Marco Polo-Images XII cruise in 2005. We are also grateful to Pham Nhu Sang for valuable discussion. We thank Editors Jimin Sun, Chenglong Deng, and Zhongshi Zhang for handling the manuscript and to three anonymous reviewers for their constructive comments on the early version of this paper. This work was financially supported by the National Natural Science Foundation of China (42130407, 42188102) and the Shanghai Science and Technology Innovation Action Plan (20590780200, 19230742100).

Appendix A. Supplementary material

This supplementary material presents the age model of Core MD05-2892, which was constructed using $\delta^{18}O$ records of *G. ruber* and AMS ^{14}C dating of planktonic foraminifera and wood debris (Supplementary Fig. S1). In addition, the supplementary material also presents the clay-mineral composition of Core MD05-2893 (Supplementary Fig. S2). Research data used in this study are available as Supplementary Table D1 in an excel file.

References

Beaulieu, E., Goddëris, Y., Donnadieu, Y., Labat, D., Roelandt, C., 2012. High sensitivity of the continental-weathering carbon dioxide sink to future climate change. Nat. Clim. Change 2, 346–349. https://doi.org/10.1038/nclimate1419.

Berner, R.A., Lasaga, A.C., Garrels, R.M., 1983. The carbonate-silicate geochemical cycle and its effect on atmospheric carbon dioxide over the past 100 million years. Am. J. Sci. 283, 641–683. https://doi.org/10.2475/ajs.283.7.641.

Brantley, S.L., Shaughnessy, A., Lebedeva, M.I., Balashov, V.N., 2023. How temperature-dependent silicate weathering acts as Earth's geological thermostat. Science 379, 382–389. https://doi.org/10.1126/science.add2922.

Cheng, H., Edwards, R.L., Sinha, A., Spötl, C., Yi, L., Chen, S., Kelly, M., Kathayat, G., Wang, X., Li, X., Kong, X., Wang, Y., Ning, Y., Zhang, H., 2016. The Asian monsoon over the past 640,000 years and ice age terminations. Nature 534, 640–646. https://doi.org/10.1038/nature18591.

Clift, P.D., Wan, S., Blusztajn, J., 2014. Reconstructing chemical weathering, physical erosion and monsoon intensity since 25 Ma in the northern South China Sea: A review of competing proxies. Earth-Sci. Rev. 130, 86–102. https://doi.org/10.1016/j.earscirev.2014.01.002.

Colin, C., Turpin, L., Blamart, D., Frank, N., Kissel, C., Duchamp, S., 2006. Evolution of weathering patterns in the Indo-Burman Ranges over the last 280 kyr: Effects of sediment provenance on $^{87}Sr/^{86}Sr$ ratios tracer. Geochem. Geophys. Geosystems 7, Q03007. https://doi.org/10.1029/2005GC000962.

Deng, K., Yang, S., Guo, Y., 2022. A global temperature control of silicate weathering intensity. Nat. Commun. 13, 1781. https://doi.org/10.1038/s41467-022-29415-0.

Dykoski, C.A., Edwards, R.L., Cheng, H., Yuan, D., Cai, Y., Zhang, M., Lin, Y., Qing, J., An, Z., Revenaugh, J., 2005. A high-resolution, absolute-dated Holocene and deglacial Asian monsoon record from Dongge Cave, China. Earth Planet. Sci. Lett. 233, 71–86. https://doi.org/10.1016/j.epsl.2005.01.036.

Galy, A., France-Lanord, C., 1999. Weathering processes in the Ganges-Brahmaputra basin and the riverine alkalinity budget. Chem. Geol. 159, 31–60. https://doi.org/10.1016/S0009-2541(99)00033-9.

Gebregiorgis, D., Giosan, L., Hathorne, E.C., Anand, P., Nilsson-Kerr, K., Plass, A., Lückge, A., Clemens, S.C., Frank, M., 2020. What can we learn from X-ray fluorescence core scanning data? A paleomonsoon case study. Geochem. Geophys. Geosystems 21, 1–17. https://doi.org/10.1029/2019GC008414.

Guo, Y., Yang, S., Su, N., Li, C., Yin, P., Wang, Z., 2018. Revisiting the effects of hydrodynamic sorting and sedimentary recycling on chemical weathering indices. Geochim. Cosmochim. Acta 227, 48–63. https://doi.org/10.1016/j.gca.2018.02.015.

Hanebuth, T.J.J., Stattegger, K., Grootes, P.M., 2000. Rapid flooding of the Sunda Shelf: A late-glacial sea-level record. Science 288, 1033–1035. https://doi.org/10.1126/science.288.5468.1033.

Hanebuth, T.J.J., Voris, H.K., Yokoyama, Y., Saito, Y., Okuno, J., 2011. Formation and fate of sedimentary depocentres on Southeast Asia's Sunda Shelf over the past sea-level cycle and biogeographic implications. Earth-Sci. Rev. 104, 92–110. https://doi.org/10.1016/j.earscirev.2010.09.006.

Hartmann, J., Jansen, N., Dürr, H.H., Kempe, S., Köhler, P., 2009. Global CO_2-consumption by chemical weathering: What is the contribution of highly active weathering regions? Glob. Planet. Change 69, 185–194. https://doi.org/10.1016/j.gloplacha.2009.07.007.

Hu, D., Böning, P., Köhler, C.M., Hillier, S., Pressling, N., Wan, S., Brumsack, H.J., Clift, P.D., 2012. Deep sea records of the continental weathering and erosion response to East Asian monsoon intensification since 14 ka in the South China Sea. Chem. Geol. 326–327, 1–18. https://doi.org/10.1016/j.chemgeo.2012.07.024.

Huang, J., Jiang, F., Wan, S., Zhang, J., Li, A., Li, T., 2016. Terrigenous supplies variability over the past 22,000 yr in the southern South China Sea slope: Relation to sea level and monsoon rainfall changes. J. Asian Earth Sci. 117, 317–327. https://doi.org/10.1016/j.jseaes.2015.12.019.

Huang, J., Wan, S., Li, A., Li, T., 2019. Two-phase structure of tropical hydroclimate during Heinrich Stadial 1 and its global implications. Quat. Sci. Rev. 222, 105900. https://doi.org/10.1016/j.quascirev.2019.105900.

Huang, X., Mei, X., Yang, S., Zhang, X., Li, F., Hohl, S. V., 2021. Disentangling combined effects of sediment sorting, provenance, and chemical weathering from a Pliocene-Pleistocene sedimentary core (CSDP-1) in the South Yellow Sea. Geochem. Geophys. Geosystems 22, e2020GC009569. https://doi.org/10.1029/2020GC009569.

Jiwarungrueangkul, T., Liu, Z., 2021. East Asian monsoon and sea-level controls on clay mineral variations in the southern South China Sea since the Last Glacial Maximum. Quat. Int. 592, 1–11. https://doi.org/10.1016/j.quaint.2021.04.033.

Jiwarungrueangkul, T., Liu, Z., Stattegger, K., Sang, P.N., 2019a. Reconstructing chemical weathering intensity in the Mekong River basin since the Last Glacial Maximum. Paleoceanogr. Paleoclimatology 34, 1710–1725. https://doi.org/10.1029/2019PA003608.

Jiwarungrueangkul, T., Liu, Z., Zhao, Y., 2019b. Terrigenous sediment input responding to sea level change and East Asian monsoon evolution since the last deglaciation in the southern South China Sea. Glob. Planet. Change 174, 127–137. https://doi.org/10.1016/j.gloplacha.2019.01.011.

Laj, C., Wang, P., Balut, Y., 2005. MD147-Marco Polo Images XII cruise report. Inst. Polaire Fr. pp. 3–11.

Lambeck, K., Rouby, H., Purcell, A., Sun, Y., Sambridge, M., 2014. Sea level and global ice volumes from the Last Glacial Maximum to the Holocene. Proc. Natl. Acad. Sci. U. S. A. 111, 15296–15303. https://doi.org/10.1073/pnas.1411762111.

Liu, Z., Colin, C., Trentesaux, A., Siani, G., Frank, N., Blamart, D., Farid, S., 2005. Late Quaternary climatic control on erosion and weathering in the eastern Tibetan Plateau and

the Mekong Basin. Quat. Res. 63, 316–328. https://doi.org/10.1016/j.yqres.2005.02.005.

Liu, Z., Colin, C., Huang, W., Phon Le, K., Tong, S., Chen, Z., Trentesaux, A., 2007. Climatic and tectonic controls on weathering in south China and Indochina Peninsula: Clay mineralogical and geochemical investigations from the Pearl, Red, and Mekong drainage basins. Geochem. Geophys. Geosystems 8, Q05005. https://doi.org/10.1029/2006GC001490.

Liu, Z., Zhao, Y., Colin, C., Siringan, F.P., Wu, Q., 2009. Chemical weathering in Luzon, Philippines from clay mineralogy and major-element geochemistry of river sediments. Appl. Geochem. 24, 2195–2205. https://doi.org/10.1016/j.apgeochem.2009.09.025.

Liu, Z., Wang, H., Hantoro, W.S., Sathiamurthy, E., Colin, C., Zhao, Y., Li, J., 2012. Climatic and tectonic controls on chemical weathering in tropical Southeast Asia (Malay Peninsula, Borneo, and Sumatra). Chem. Geol. 291, 1–12. https://doi.org/10.1016/j.chemgeo.2011.11.015.

Liu, Z., Zhao, Y., Colin, C., Stattegger, K., Wiesner, M.G., Huh, C.A., Zhang, Y., Li, X., Sompongchaiyakul, P., You, C.F., Huang, C.Y., Liu, J.T., Siringan, F.P., Le, K.P., Sathiamurthy, E., Hantoro, W.S., Liu, J., Tuo, S., Zhao, S., Zhou, S., He, Z., Wang, Y., Bunsomboonsakul, S., Li, Y., 2016. Source-to-sink transport processes of fluvial sediments in the South China Sea. Earth-Sci. Rev. 153, 238–273. https://doi.org/10.1016/j.earscirev.2015.08.005.

Lupker, M., France-Lanord, C., Galy, V., Lavé, J.Ô., Kudrass, H., 2013. Increasing chemical weathering in the Himalayan system since the Last Glacial Maximum. Earth Planet. Sci. Lett. 365, 243–252. https://doi.org/10.1016/j.epsl.2013.01.038.

Milliman, J.D., Syvitski, J.P.M., 1992. Geomorphic/tectonic control of sediment discharge to the ocean: The importance of small mountainous rivers. J. Geol. 100, 525–544. https://doi.org/10.1086/629606.

Milliman, J.D., Farnsworth, K.L., Albertin, C.S., 1999. Flux and fate of fluvial sediments leaving large islands in the East Indies. J. Sea Res. 41, 97–107. https://doi.org/10.1016/S1385-1101(98)00040-9.

Molengraaff, G.A.F., Weber, M., 1921. On the relation between the Pleistocene glacial period and the origin of the Sunda Sea (Java and South China Sea), and its influence on the distribution of coral reefs and on the land and freshwater fauna. Proceeding R. Acad. Amst. 23, 395–439.

Nesbitt, H.W., Young, G.M., 1982. Early Proterozoic climates and plate motions inferred from major element chemistry of lutites. Nature 299, 715–717. https://doi.org/10.1038/299715a0.

Parker, A., 1970. An index of weathering for silicate rocks. Geol. Mag. 107, 501–504. https://doi.org/10.1017/S0016756800058581.

Partin, J.W., Cobb, K.M., Adkins, J.F., Clark, B., Fernandez, D.P., 2007. Millennial-scale trends in west Pacific warm pool hydrology since the Last Glacial Maximum. Nature 449, 452–455. https:// doi.org/10.1038/nature06164.

Sang, P.N., Liu, Z., Stattegger, K., 2019. Weathering and erosion in central Vietnam over the Holocene and Younger Dryas: Clay mineralogy and elemental geochemistry from the Vietnam Shelf, western South China Sea. J. Asian Earth Sci. 179, 1–10. https://doi.org/10.1016/j.jseaes.2019.04.008.

Sang, P.N., Liu, Z., Colin, C., 2022. Chemical weathering of the Mekong River basin with implication for East Asian monsoon evolution during the late Quaternary: Marine sediment records in the southern South China Sea. Front. Earth Sci. 10, 885547. https://doi.org/10.3389/feart.2022.885547.

Sathiamurthy, E., Voris, H., 2006. Maps of Holocene sea level transgression and submerged lakes on the Sunda Shelf. Nat. Hist. J. Chulalongkorn Univ. Supplement 2, 1–44.

Steinke, S., Kienast, M., Hanebuth, T., 2003. On the significance of sea-level variations and shelf paleo-morphology in governing sedimentation in the southern South China Sea during the last deglaciation. Mar. Geol. 201, 179–206. https://doi.org/10.1016/S0025-3227(03)00216-0.

Steinke, S., Hanebuth, T.J.J., Vogt, C., Stattegger, K., 2008. Sea level induced variations in clay mineral composition in the southwestern South China Sea over the past 17,000 yr. Mar. Geol. 250, 199–210. https://doi.org/10.1016/j.margeo.2008.01.005.

Stuiver, M., Grootes, P.M., Braziunas, T., 1995. The GISP2 $\delta^{18}O$ climate record of the past 16,500 years and the role of the Sun, ocean, and volcanoes. Quat. Res. 44, 341–354. https://doi.org/10.1006/qres.1995.1079.

Sun, X., Li, X., Luo, Y., Chen, X., 2000. The vegetation and climate at the last glaciation on the emerged continental shelf of the South China Sea. Palaeogeogr. Palaeoclimatol. Palaeoecol. 160, 301–316. https://doi.org/10.1016/S0031-0182(00)00078-X.

Sun, Y., Oppo, D.W., Xiang, R., Liu, W., Gao, S., 2005. Last deglaciation in the Okinawa Trough: Subtropical northwest Pacific link to Northern Hemisphere and tropical climate. Paleoceanography 20, PA4005. https://doi.org/10.1029/2004PA001061.

Voris, H.K., 2000. Maps of Pleistocene sea levels in Southeast Asia: Shorelines, river systems and time durations. J. Biogeogr. 27, 1153–1167. https://doi.org/10.1046/j.1365-2699.2000.00489.x.

Wan, S., Clift, P.D., Zhao, D., Hovius, N., Munhoven, G., France-Lanord, C., Wang, Y.,

Xiong, Z., Huang, J., Yu, Z., Zhang, J., Ma, W., Zhang, G., Li, A., Li, T., 2017. Enhanced silicate weathering of tropical shelf sediments exposed during glacial lowstands: A sink for atmospheric CO_2. Geochim. Cosmochim. Acta 200, 123–144. https://doi.org/10.1016/j.gca.2016.12.010.

Wang, Y., Cheng, H., Edwards, R.L., An, Z., Wu, J., Shen, C., Dorale, J.A., 2001. A high-resolution absolute-dated late Pleistocene monsoon record from Hulu Cave, China. Science 294, 2345–2348. https://doi.org/10.1126/science.1064618.

Xie, X., Zheng, H.B., Qiao, P.J., 2014. Millennial climate changes since MIS 3 revealed by element records in deep-sea sediments from northern South China Sea. Chin. Sci. Bull. 59, 776–784. https://doi.org/10.1007/s11434-014-0117-9.

Xu, Z., Li, T., Clift, P.D., Wan, S., Qiu, X., Lim, D., 2017. Barium records of enhanced silicate erosion and weathering on the exposed Luzon shelf during glacial lowstands and their significance for atmospheric CO_2 sink. Chem. Geol. 476, 302–315. https://doi:10.1016/j.chemgeo.2017.11.027.

Yu, Z., Tang, X., Colin, C., Wilson, D.J., Zhou, X., Song, L., Chang, F., Zhang, S., Bassinot, F., Wan, S., 2023. Millennial-scale precipitation variability in the Indo-Pacific region over the last 40 Kyr. Geophys. Res. Lett. 50, e2022GL101646. https://doi.org/10.1029/2022GL101646.

Zhao, H., Liu, Z., Zhao, Y., Wu, J., Colin, C., 2023. Lunar nodal tidal cycle influences on the input of coarse sediments during the last glaciation in the deep South China Sea. Quat. Sci. Rev. 310, 108114. https://doi.org/10.1016/j.quascirev.2023.108114.

Zhao, M., Huang, C., Wang, C., Wei, G., 2006. A millennial-scale $U^{K'}_{37}$ sea-surface temperature record from the South China Sea (8°N) over the last 150 kyr: Monsoon and sea-level influence. Palaeogeogr. Palaeoclimatol. Palaeoecol. 236, 39–55. https://doi.org/10.1016/j.palaeo.2005.11.033.

Declaration of interests

The authors declare that they have no known competing financial interests or personal relationships that could have appeared to influence the work reported in this paper.

Highlights

- Provenance of sediments off the Sunda Shelf has changed from glaciation to Holocene

- Intensive chemical weathering occurred on Malay Peninsula/Sumatra during glaciation
- Sea level and East Asian monsoon have jointly affected deep-sea weathering records